Articles

The Novel Binding Mode of *N*-Alkyl-*N*′-hydroxyguanidine to Neuronal Nitric Oxide Synthase Provides Mechanistic Insights into NO Biosynthesis†

Huiying Li,‡ Hideaki Shimizu,‡ Mack Flinspach,‡ Joumana Jamal,‡ Weiping Yang,‡ Ming Xian,§ Tingwei Cai,§ Edward Zhong Wen,§ Qiang Jia,§ Peng George Wang,§ and Thomas L. Poulos*,‡

Department of Molecular Biology and Biochemistry and Program in Macromolecular Structures, University of California, Irvine, California 92697, and Department of Chemistry, Wayne State University, Detroit, Michigan 48202

Received June 13, 2002; Revised Manuscript Received August 30, 2002

ABSTRACT: A series of *N*-alkyl-*N*′-hydroxyguanidine compounds have recently been characterized as non-amino acid substrates for all three nitric oxide synthase (NOS) isoforms which mimic NO formation from N^{ω}-hydroxy-L-arginine. Crystal structures of the nNOS heme domain complexed with either *N*-isopropyl-*N*′-hydroxyguanidine or *N*-butyl-*N*′-hydroxyguanidine reveal two different binding modes in the substrate binding pocket. The binding mode of the latter is consistent with that observed for the substrate N^{ω}-hydroxy-L-arginine bound in the nNOS active site. However, the former binds to nNOS in an unexpected fashion, thus providing new insights into the mechanism on how the hydroxyguanidine moiety leads to NO formation. Structural features of substrate binding support the view that the OH-substituted guanidine nitrogen, instead of the hydroxyl oxygen, is the source of hydrogen supplied to the active ferric−superoxy species for the second step of the NOS catalytic reaction.

Nitric oxide synthases (NOSs)[1] are a class of enzymes found in mammals and other species that utilize L-arginine to generate NO, an important signaling molecule involved in a wide range of physiological functions as well as pathophysiological states (*1*−*4*). Three NOS isoforms identified in various mammalian cells, neuronal NOS, inducible NOS, and endothelial NOS, catalyze the same reactions in the following two consecutive steps with O_2 and NADPH as the cosubstrates:

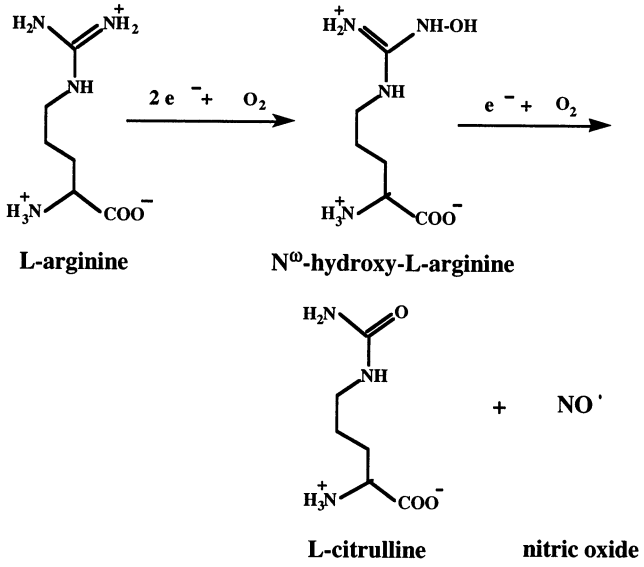

L-Arg is first hydroxylated to N^{ω}-hydroxy-L-arginine (L-NHA), which is then further converted to NO and L-citrulline (*5*, *6*). Both steps occur at the same heme active site, although the active catalytic species are believed to be different. The initial hydroxylation of L-Arg is thought to utilize a P450-like Fe(IV)−O species as the active hydroxylating species, while the second step, L-NHA to L-citrulline and NO, is thought to use an Fe(III)−hydroperoxy species (*7*). Another unique feature in NOS catalysis is the requirement for tetrahydrobiopterin, H_4B, in both steps of the reaction. H_4B now is thought to play an essential redox role by providing an electron required to activate the Fe(II)−oxy complex to the active hydroxylating species, Fe(IV)−O or Fe(III)−hydroperoxy (*8*, *9*). Direct experimental support for a redox role of H_4B stems from freeze quench EPR which has shown that an H_4B does indeed form a radical when L-Arg is oxidized to L-NHA (*10*−*12*).

NOS is a complex molecule consisting of an N-terminal heme domain containing the active site and a C-terminal FAD/FMN domain that serves as the source of electrons required for substrate oxidation in the heme domain (*13*).

† This work was supported by NIH Grants GM57353 (T.L.P.) and GM54074 (P.G.W.).

* To whom correspondence should be addressed. E-mail: poulos@uci.edu. Telephone: (949) 824-7020. Fax: (949) 824-3280.

‡ University of California.

§ Wayne State University.

[1] Abbreviations: NOS, nitric oxide synthase; L-Arg, L-arginine; L-NHA, N^{ω}-hydroxy-L-arginine; H_4B, (6*R*)-5,6,7,8-tetrahydro-L-biopterin; IHA, N^{ω}-isopropyl-$N^{\omega\prime}$-hydroxyarginine; IHG, *N*-isopropyl-*N*′-hydroxyguanidine; BHG, *N*-butyl-*N*′-hydroxyguanidine; IPTG, isopropyl β-D-thiogalactopyranoside; PMSF, phenylmethanesulfonyl fluoride; NTA, nitrilotriacetic acid; GSH, glutathione (reduced form); SDS, sodium dodecyl sulfate.

10.1021/bi020417c CCC: $22.00
Published on Web 10/30/2002

Chart 1

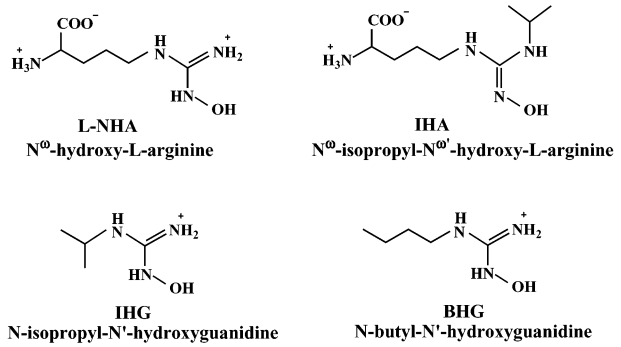

Electrons are funneled from NADPH via FAD and FMN to the heme (*7*). The heme−flavin domain interaction and hence, electron transfer, is regulated by calmodulin (*14*). Structural work to date has focused on the heme domain alone. The crystal structures of the catalytic heme domain of the three NOS isoforms (*15*−*17*) (that of nNOS to be published) show that the substrate binding site on the distal side of the heme plane is nearly identical. As with P450s, the substrate is held in place by a series of protein−substrate interactions such that the atom to be hydroxylated, in this case an L-Arg guanidinium N atom, is positioned directly adjacent to the iron-bound oxygen. It would appear that any molecule that can bind to NOS with a guanidinium group similarly positioned should serve as a NOS substrate. This, however, is not the case. The first hydroxylation step is quite specific for L-Arg, although homo-L-Arg (one methylene group longer than L-Arg) also is a substrate (*18*). This implies that the NOS substrate needs not only a guanidinium moiety but also an amino acid headgroup to satisfy the extensive H-bonding networks observed in the crystal structures that help to define the highly specific enzyme−substrate interactions for L-Arg and its derivatives. However, the second step of the reaction is much less specific. Recently, a series of N-substituted *N*′-hydroxyguanidine compounds (*19*−*21*) which mimic L-NHA have been found to serve as efficient substrates in NO formation. These hydroxyguanidines generate NO through an enzymatic process requiring a fully functional NOS electron transfer machinery consisting of NADPH, H_4B, and calmodulin. These hydroxyguanidines are not only good substrates, but some display significant isoform selection as well. The ability to selectively promote NO formation using isoform-selective substrates could have potential therapeutic value. To better understand how these substrates interact with NOS, we have determined the crystal structures of nNOS complexed with *N*-isopropyl-*N*′-hydroxyguanidine (IHG, Chart 1) and *N*-butyl-*N*′-hydroxyguanidine (BHG) in comparison with that of *N*$^{\omega}$-hydroxy-L-arginine (L-NHA). The unexpected binding mode of IHG in the active site provides new insights into the mechanism of hydroxyguanidine oxidation for generating NO.

MATERIALS AND METHODS

Materials. Reagents used in organic synthesis were obtained from Aldrich. L-NHA and H_4B was purchased from Alexis. Lysozyme, IPTG, pepstatin A, leupeptin, antipain, and other chemicals used in the purification buffer were obtained from Sigma. Sucrose, trehalose, and mannitol were from CalBiochem. Both *N*-isopropyl-*N*′-hydroxyguanidine and *N*-butyl-*N*′-hydroxyguanidine were synthesized according to the procedures reported previously (*21*).

Scheme 1

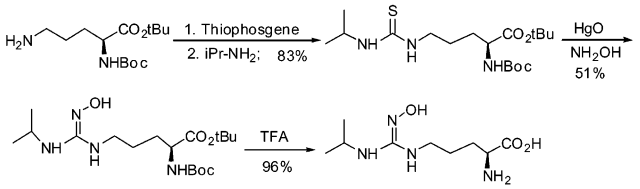

Synthesis of N$^{\omega}$*-Isopropyl-N*$^{\omega'}$*-hydroxy-*L*-arginine.* N$^{\omega}$-Isopropyl-N$^{\omega'}$-hydroxy-L-arginine was prepared on the basis of a published method (*22*) with modification (Scheme 1).

(1) N$^{\alpha}$*-(tert-Butyloxycarbonyl)-δ-(N-isopropylthioureido)-*L*-norvaline tert-Butyl Ester*. N$^{\alpha}$-(*tert*-Butyloxycarbonyl)-L-ornithine *tert*-butyl ester (5 mmol), thiophosgene (15 mmol), and calcium carbonate (5.15 mmol) in 40 mL of chloroform and 5 mL of water were stirred vigorously for 16 h. The suspension was filtered, and the organic layer was separated. After concentration, the residue was dissolved in 20 mL of methanol and cooled in an ice bath. Isopropylamine (50 mmol) was added, and then the mixture was stirred for 3 h at room temperature. Evaporation and purification with silica gel chromatography (4:1 EtOAc/hexane) afforded a white solid (1.617 g, 83%): ^{1}H NMR (400 MHz, $CDCl_3$) δ 6.51 (broad, 1H), 6.09 (broad, 1H), 5.21 (d, $J = 8$ Hz, 1H), 4.22 (broad, 1H), 4.04−4.06 (m, 1H), 3.44 (m, 2H), 1.8−1.5 (m, 4H), 1.41 (s, 9H), 1.38, (s, 9H), 1.16 (d, $J = 8$ Hz, 6H); ^{13}C NMR (400 MHz, $CDCl_3$) δ 180.5, 171.8, 155.9, 82.6, 80.2, 53.5, 46.1, 43.9, 30.9, 28.7, 28.5, 28.2, 25.0, 22.8; ESI-MS 390 ($M^+ + 1$).

(2) N$^{\alpha}$*-(tert-Butyloxycarbonyl)-N*$^{\omega}$*-isopropyl-N*$^{\omega'}$*-hydroxy-*L*-arginine tert-Butyl Ester*. Triethylamine (3 mL) was added to a stirred mixture of 0.55 mmol of N$^{\alpha}$-(*tert*-butyloxycarbonyl)-δ-(*N*-isopropylthioureido)-L-norvaline *tert*-butyl ester, 120 mg of HgO, and 38 mg of hydroxylamine hydrochloride under a nitrogen atmosphere. The mixture was extracted with diethyl ether overnight and was subjected to silica gel column chromatography with chloroform and methanol (10:1) as the eluent to give the desired compound as an oil (83.6 mg, 39%): ^{1}H NMR (500 MHz, CD_3OD) δ 4.30 (broad, 1H), 3.96 (broad t, 1H), 3.46 (broad, 2H), 1.80−1.55 (m, 4H), 1.46 (s, 9H), 1.44, (s, 9H), 1.17 (d, $J = 6.5$ Hz, 6H); ^{13}C NMR (500 MHz, CD_3OD) δ 172.4, 156.9, 81.4, 79.3, 54.5, 43.3, 28.9, 27.6, 27.1, 25.7, 21.5.

(3) N$^{\omega}$*-Isopropyl-N*$^{\omega'}$*-hydroxy-*L*-arginine*. N$^{\alpha}$-(*tert*-Butyloxycarbonyl)-N$^{\omega}$-isopropyl-N$^{\omega'}$-hydroxy-L-arginine *tert*-butyl ester (83.6 mg) was stirred in 10 mL of trifluoroacetic acid for 2 h. After evaporation in vacuo, 10 mL of water and 10 mL of ether were added. The water layer was separated and lyophilized. The final was a white solid (50 mg, >99%): ^{1}H NMR (300 MHz, CD_3OD) δ 3.93 (t, 1H), 3.77 (sept, 1H), 3.15 (dt, 2H), 2.0−1.5 (m, 4H), 1.09 (d, $J = 8$ Hz, 6H); ^{13}C NMR (300 MHz, D_2O) δ 171.9, 52.7, 46.8, 43.2, 27.1, 24.3, 21.4, 8.4; ESI-MS 233 ($M^+ + 1$). The purity of the product was further confirmed by HPLC using a C-18 column and water and CH_3CN (80:20) as the eluent. Structures of the three compounds synthesized for this study are shown in Chart 1.

Expression and Purification of nNOS. The plasmid encoding rat brain nNOS, pHis/nNOS, was a generous gift from

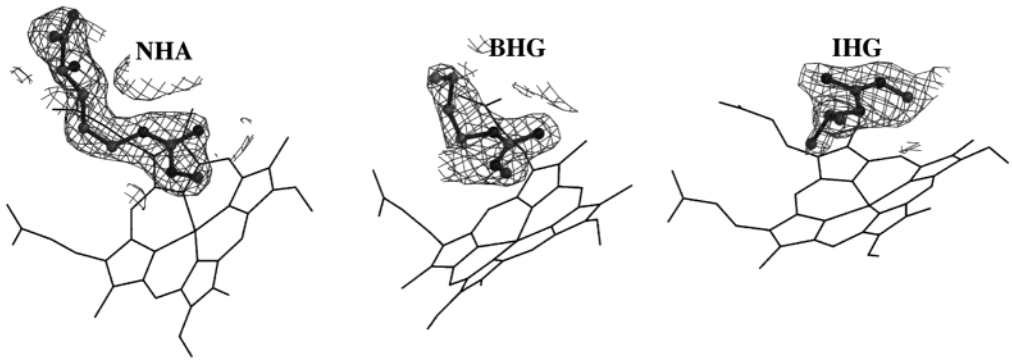

FIGURE 1: Omit maps ($2F_o - F_c$) contoured at 1σ for the three complex structures. The ligand that was labeled was omitted during each calculation using a simulated annealing protocol in CNS. The figure was made with BOBSCRIPT (*39*) and RASTER3D (*40*).

P. Ortiz de Montellano (*23*). The rat nNOS gene was subcloned into the *Nde*I and *Xba*I sites of a pCWori vector which also bears the *Amp*^{R} gene and an N-terminal six-His tag. The holo-nNOS was expressed in *Escherichia coli* strain BL21(DE3) and cultured in TB medium (100 μg/mL ampicillin, 1 L in each 2.8 L Fernbach flask) at 37 °C with agitation at 250 rpm until the OD (600 nm) reached 1.0−1.2. Protein expression was then induced by adding 0.7 mM IPTG. Cell growth was continued at 25 °C and 150 rpm for 40 h. Cells were harvested by centrifugation and stored at −70 °C.

The major components of the buffer used for purification were 50 mM Tris-HCl (pH 7.9), 10% glycerol, 5 mM βME, 0.5 mM L-Arg, 10 μM H_4B, 0.1 mM PMSF, and protease inhibitors pepstatin A, leupeptin, and antipain (1 μg/mL each). This buffer will be called buffer A. The cell paste was resuspended with buffer A plus 200 mM NaCl and 1 mg/mL lysozyme followed by sonication. Cell debris was removed by ultracentrifugation at ~100000*g* for 1 h. The cell-free extract was loaded onto a 20 mL Ni NTA column (Qiagen) which had been equilibrated with 10 bed volumes of buffer A plus 200 mM NaCl. After the sample had been loaded, the column was washed with 10 bed volumes of buffer A plus 500 mM NaCl and 5 mM imidazole. Elution was achieved with a 5 to 200 mM imidazole linear gradient in buffer A plus 500 mM NaCl. Colored fractions were pooled and concentrated with a CentriPrep 30 apparatus to a small volume before being loaded onto a Superdex 200 column (HiLoad 26/60, Amersham Pharmacia) which was controlled by an FPLC system. The running buffer for this column was buffer A plus 200 mM NaCl. When substrate-free nNOS was desired, 0.5 mM L-Arg in buffer A was replaced with 5 mM imidazole.

To generate the heme domain of nNOS used for crystallization, the purified holo-nNOS sample was subjected to trypsinolysis on ice for 1 h at an nNOS:trypsin weight ratio of 100:1. The digested sample was loaded onto a Superdex 200 column again to separate the nNOS heme domain from a flavin-containing fragment generated by trypsin cleavage. The first residue of the heme domain of nNOS was identified as Cys297 by the N-terminal amino acid sequencing at the core facility of the University of California (Irvine, CA).

Crystallization. The crystallization conditions for the nNOS heme domain complexed with various ligands are essentially the same as those that have been described elsewhere for the nNOS substrate complex (to be published). In general, 5−8 mM ligand was added to the nNOS protein sample (at 7−9 mg/mL with 5 mM imidazole) prior to setting up sitting drops. According to the particular ligand used in the cocrystallization, the ingredients of the crystallization cocktail have to be fine-tuned within the following range: 18−22% (w/v) PEG 3350, 0.1 M MES (pH 5.6−6.0), and 100−200 mM ammonium acetate. In addition, 2.0 mM GSH and 35 μM SDS remained constant. Crystals reached full size at 5 °C in 2 days. The cryoprotectants used for cryogenic data collection include 10% glycerol, 10% trehalose, and sucrose and mannitol (5% each).

X-ray Diffraction Data Collection, Processing, and Structure Refinement. X-ray diffraction data of the nNOS heme domain were collected at beamline BL7-1 of the Stanford Synchrotron Radiation Laboratory (Stanford, CA) with a Mar345 image plate. Data frames were processed using HKL (*24*). The binding of ligand was detected by a difference Fourier technique using CNS (*25*) with a refined, ligand- and water-removed nNOS heme domain structure as the starting model (PDB entry 1K2Q). Once the new ligand was modeled into the electron density with O (*26*), structures were further refined with CNS and water molecules were added using the waterpick routine in CNS and visually inspected in O. The maximum likelihood target function was used for the refinement with all the observed reflections included in the calculations. The ligand binding was also confirmed toward the end of the refinement by calculating omit maps with a simulated annealing protocol at a starting temperature of 1000 K. The omit electron density maps for the ligands in all three complexes are shown in Figure 1. Data collection and refinement statistics are summarized in Table 1.

RESULTS

N^ω-Hydroxy-L-arginine (L-NHA) Complex. L-NHA binds to the nNOS active site in a fashion similar to that of L-Arg, shown in Figure 2A. The protein−ligand interactions can be divided into two sites. One is the amino acid binding pocket where one of the carboxylate oxygen atoms of L-NHA accepts H-bonds from Tyr588 and Gln478 and the other carboxylate oxygen is within H-bonding distance of Asp597. The α-amino nitrogen forms H-bonds forming a bridge between the Glu592 side chain and one of the heme propionates. The amino acid binding pocket is specific for the L-enantiomer since the configuration of carboxylate and α-amino groups in a D-isomer cannot satisfy all H-bonding interactions with the protein as observed for the L-isomer. The second site is right above the heme plane where the guanidine group maintains three hydrogen bonds via its

Table 1: Data Collection and Refinement Statistics[a]

	NHA	IHG	BHG
PDB entry	1LZX	1LZZ	1M00
cell dimensions (Å)	$a = 51.93$	$a = 52.02$	$a = 52.07$
(space group $P2_12_12_1$)	$b = 110.74$	$b = 111.11$	$b = 111.25$
	$c = 164.73$	$c = 163.78$	$c = 163.84$
data resolution (Å)	2.00	2.05	2.05
no. of total observations	208445	202846	173591
no. of unique reflections	62410	59070	58402
R_{sym}[b]	0.069 (0.780)[c]	0.071 (0.616)	0.079 (0.621)
$\langle I/\sigma \rangle$	8.8 (2.1)[c]	8.8 (1.8)	9.0 (1.5)
completeness	0.961 (0.925)[c]	0.976 (0.926)	0.954 (0.907)
no. of reflections in refinement	62363	59007	57951
R_{factor}[d]	0.226	0.226	0.229
R_{free}[e]	0.256	0.266	0.270
no. of protein atoms	6655	6655	6655
no. of heteroatoms	155	145	147
no. of waters	469	511	498
rms deviation			
bond lengths (Å)	0.007	0.008	0.011
bond angles (deg)	1.3	1.4	1.5

[a] NHA, N^{ω}-hydroxy-L-arginine; IHG, *N*-isopropyl-*N*′-hydroxyguanidine; BHG, *N*-butyl-*N*′-hydroxyguanidine. [b] $R_{sym} = \sum|I - \langle I \rangle|/\sum I$, where I is the observed intensity and $\langle I \rangle$ the averaged intensity of multiple symmetry-related observations of the reflection. [c] The values in parentheses were obtained in the outermost resolution shell. [d] $R_{factor} = \sum||F_o| - |F_c||/\sum|F_o|$, where F_o and F_c are the observed and calculated structure factors, respectively. [e] R_{free} was calculated with the 5% of reflections set aside randomly throughout the refinement. The same set of reflections was chosen for every data set.

bridging nitrogen (NE according to PDB nomenclature) and its unsubstituted terminal nitrogen (NH2) to the Glu592 side chain and the Trp587 carbonyl oxygen. The hydroxyl group of L-NHA does not coordinate the heme iron but instead points away from the iron toward the backbone amide of Gly586 to form a weak H-bond or nonbonded contact. The OH group tilts by 15−30° from the guanidino plane, most likely due to the protein−ligand interaction in the active site. The L-NHA binding mode in nNOS is essentially identical to what has been reported for human eNOS (*16*) and murine iNOS (*27*). The subtle difference is that the L-NHA bound in human eNOS has its OH group coplanar with the guanidino nitrogen atoms, which was also observed in an L-NHA-bound bovine eNOS structure (PDB entry 5NSE; C. S. Raman, H. Li, P. Martasek, B. S. S. Masters, and T. L. Poulos, unpublished results). Why the hydroxyguanidine moiety is planar in eNOS but nonplanar in iNOS or nnNOS is not clear.

N-Butyl-N′-hydroxyguanidine (BHG) Complex. The orientation of the guanidino plane of *N*-butyl-*N*′-hydroxyguanidine (BHG) found at the nNOS active site is similar to that of L-NHA (Figure 2B). For comparison purposes, the atom nomenclature in the guanidine group of hydroxyguanidine compounds is kept the same as that in L-NHA. The guanidine moiety of BHG is hydrogen-bonded to the Glu592 side chain and Trp587 carbonyl oxygen like the L-NHA complex. Also like L-NHA, the BHG OH group points toward the backbone amide of Gly587 with a tilt angle of 16° from the guanidino plane. The main difference between BHG and NHA is the location of the butyl group in BHG compared to the methylene carbons of NHA. The end of the butyl group curls toward Gln478 and Val567 away from the binding site for the substrate or NHA α-amino and carboxylate groups. The side chain of Gln478 has to swing away slightly to avoid close van der Waals contact to the ligand, while the butyl group is ∼3.7 Å from Val567 which probably provides favorable nonbonded interactions.

N-Isopropyl-N′-hydroxyguanidine (IHG) Complex. The binding mode of *N*-isopropyl-*N*′-hydroxyguanidine (IHG) was totally unexpected. In this case, the isopropyl-attached NE atom takes the position normally occupied by the OH-substituted terminal nitrogen NH1 in the other two complexes (Figure 2C). Two methyl groups of the isopropyl moiety make favorable van der Waals contacts with side chains of both Val567 and Phe584. This ligand orientation places the OH group into the corner between the Glu592 carboxylate and the Trp587 carbonyl. The OH oxygen atom is only 2.48 Å from the Trp587 carbonyl oxygen, while both NH1 and NH2 atoms of guanidine are involved in the bifurcate H-bonds with the Glu592 carboxylate oxygen atoms. To accommodate the OH group in this narrow corner, the guanidino plane of IHG is shifted slightly away from the β-strand where Trp587 resides compared to the position normally observed for L-NHA or BHG. The OH group also bends downward toward the heme by 15° from the guanidino plane. In the process of validating the current model of IHG, we did notice in the omit map some extended feature on the side of the unsubstituted NH2 atom. Swapping the positions of NH1 (OH attached) and NH2 was attempted to test if the extended feature is due to the OH adapting an alternate position. However, in this alternate model, serious steric clashing occurs between the OH and isopropyl groups. Although this alternate binding mode of IHG is not totally impossible, it is at least not energetically favorable. The extended feature on the side of NH2 might be attributed to an H-bonded water molecule. However, with the electron density calculated at 2.05 Å resolution, a water molecule can only be placed next to the NH2 atom in one of the two subunits in the structure.

Properties of N^{ω}-Isopropyl-$N^{\omega\prime}$-hydroxy-L-arginine (IHA). The novel binding mode of IHG prompted us to synthesize its amino acid counterpart, N^{ω}-isopropyl-$N^{\omega\prime}$-hydroxy-L-arginine (IHA), and characterize its behavior. On the basis of the oxyhemoglobin assay (*21*), this compound was found not to be a substrate for nNOS and iNOS (data not shown). A spectral titration with IHA of the imidazole-bound (1 mM) nNOS heme domain (data not shown) revealed no high-spin shift of the 427 nm peak with up to 3.5 mM ligand, indicating a low affinity for nNOS. The reason that IHA cannot bind well to the NOS active site is very likely due to the incompatibility of satisfying the H-bonding interactions of the amino acid carboxylate and amino groups on one end of the compound and interactions from the protein to both isopropyl and OH groups attached to the guanidino group on the other end. In other words, both sets of interactions cannot be satisfied simultaneously which would force one end or the other to adopt an unfavorable conformation and poor contacts with the protein.

DISCUSSION

Binding Mode of Related Compounds. Before the main mechanistic implications of this work are considered, it is worth reviewing what is known about various inhibitors and substrates related to those that are the topic of this work.

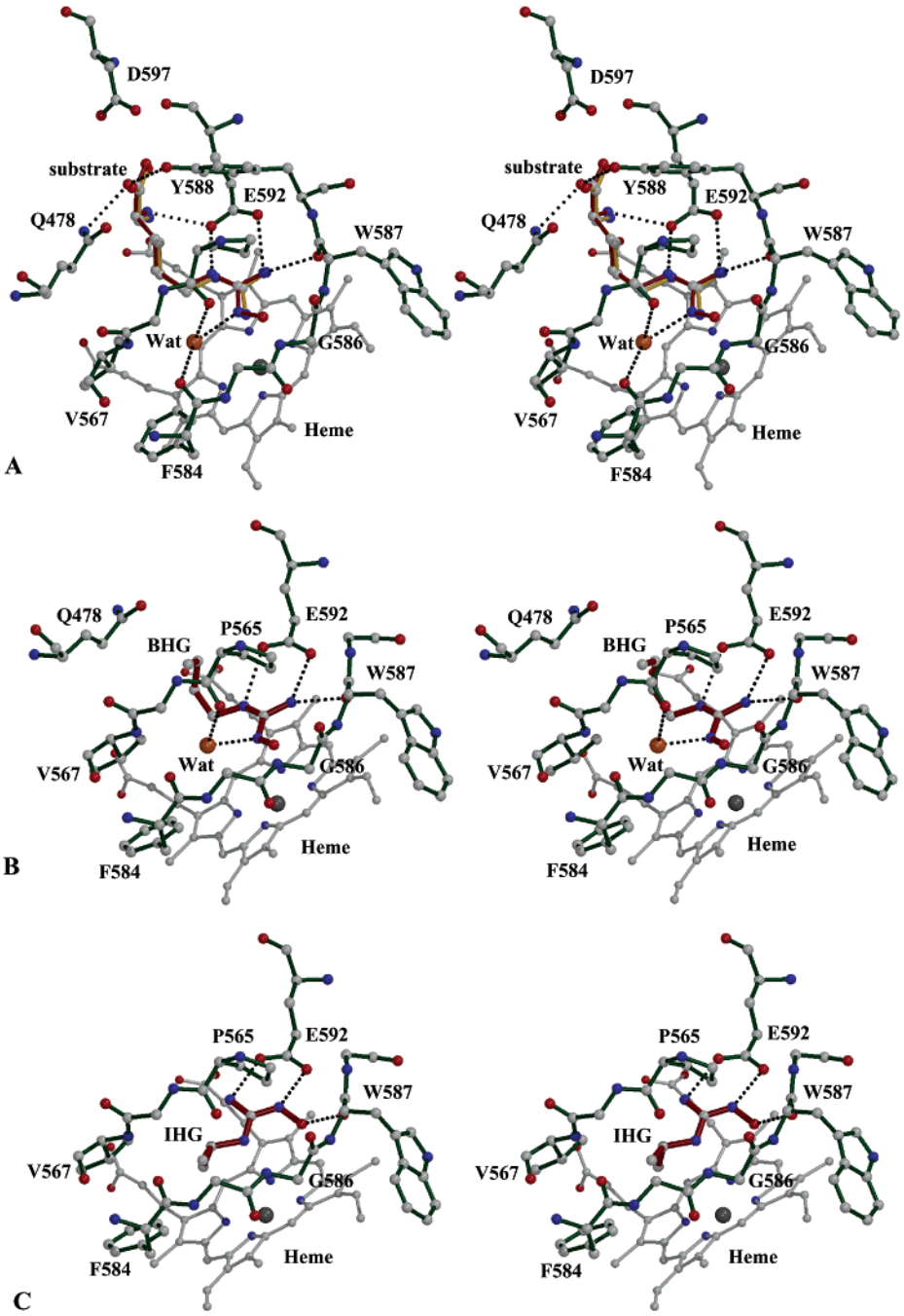

FIGURE 2: Stereoviews of the ligand-bound nNOS active site: (A) L-NHA (dark red) with L-Arg (gold) superimposed, (B) *N*-butyl-*N*′-hydroxyguanidine (BHG), and (C) *N*-isopropyl-*N*′-hydroxyguanidine (IHG). H-Bonds are drawn as dotted lines. The atomic color scheme used for amino acids is as follows: gray for carbon, red for oxygen, and blue for nitrogen. This figure was prepared with MOLSCRIPT (*41*) and RASTER3D (*40*).

Well before the NOS crystal structures became available it was known that asymmetric dimethylarginine (ADMA) where both methyl groups are attached to one guanidino N atom is an inhibitor of NOS, but that symmetric dimethylarginine (SDMA) where each methyl group is attached to a different N atom is not (*28*, *29*). This was clearly explained by the binding mode of L-Arg and its analogues in the NOS active site revealed by the crystal structures. Although the two terminal guanidino nitrogens are chemically equivalent when the guanidinium is charged, the binding environments of each N atom in the active site are quite distinct. One terminal nitrogen (NH2), with two hydrogens attached, donates H-bonds to both the Glu592 side chain and the carbonyl oxygen of Trp587 in a rather narrow corner. The other terminal nitrogen (NH1) is pointing toward an open space where it contacts the protein only through a bridging water molecule. Presumably, this is the N atom which is hydroxylated in the first step of NO synthesis. Apparently, this nitrogen has enough room to accommodate small substituents, such as small alkyl, nitro, and amino groups which give rise to many amino acid-based inhibitors (Figure 3). In contrast, the corner of the active site around the terminal nitrogen NH2 is so congested that even a methyl group cannot be tolerated. This is the reason that SDMA is not an inhibitor and, possibly why in our current study, we find that IHA is not a substrate and cannot bind to nNOS

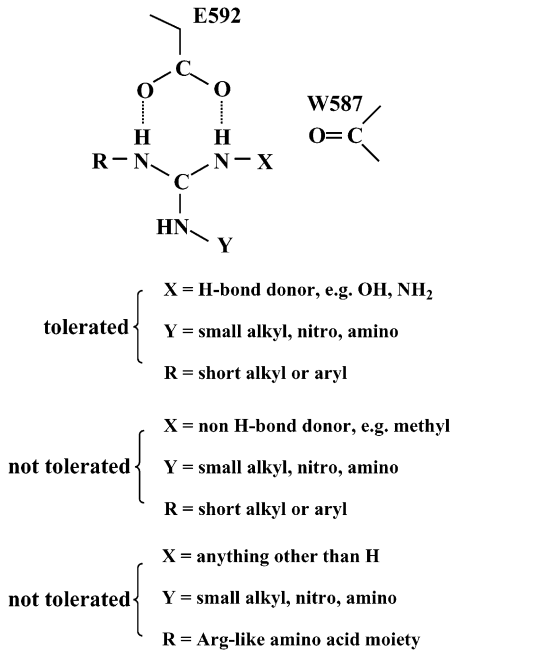

FIGURE 3: Schematic illustration of tolerated substituents on the two terminal guanidino nitrogen atoms when the L-arginine or guanidine derivatives are bound at the NOS active site. Note that a small H-bond donor group is tolerated in the X position when the R group is a less bulky alkyl or aryl group; in contrast, nothing but H is allowed in the X position when the R group is an L-amino acid moiety that occupies the specific L-amino acid binding pocket in the NOS active site.

Chart 2

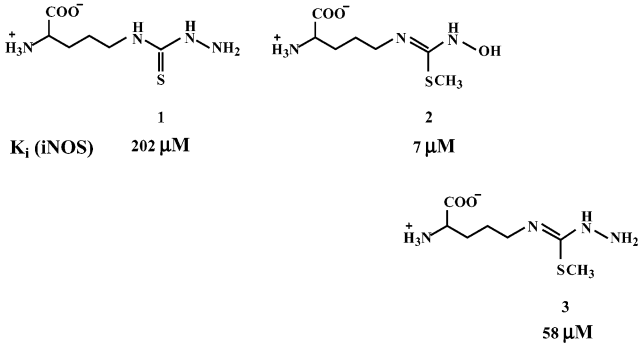

well enough to be detected using the traditional low-to-high spin shift assay.

Griffith and co-workers (*30*) synthesized a series of L-Arg analogues with either terminally substituted guanidines, or amidines where one of the terminal nitrogens is replaced with a carbon, or thioureas where one of the terminal nitrogens becomes sulfur. The resulting binding data indicate that the binding pocket of the terminal guanidinium nitrogen NH2 has a strong preference for $-NH_2$ and $=NH_2^+$ groups, but with a decreasing affinity for $=S$, $=O$, and $-CH_3$ groups, whereas the environments of the terminal nitrogen NH1 favors $=S$ (and $-S$-alkyl), $=O$, alkyl, $-NH$-alkyl, and $-NH_2$ or $=NH_2^+$ groups, in descending order.

Further evidence of what can be tolerated in the narrow corner of the terminal guanidino nitrogen NH2 was provided by King's lab (*31*) with a series of sulfur-containing L-arginine-derived inhibitors (Chart 2). Although nonpolar substituents as small as a methyl group are not allowed on the terminal nitrogen NH2, polar ones such as OH and NH_2 are tolerated (Figure 3). The thiourea or isothiourea compounds **1**, **2**, and **3** in Chart 2 are competitive inhibitors for all three NOS isoforms. The NH-OH group fits better than the NH-NH_2 group since compound **2** has the lowest K_i value among the series. Due to the presence of an H-bond acceptor, the carbonyl oxygen of Trp587 is considered, having a hydrogen-donating group like OH or NH_2 as the terminal nitrogen substituent contributes favorably to ligand binding. The inability to H-bond might be the reason for the intolerance to a methyl group at this position because nonbonded contacts demand more space than H-bonded interactions.

Here in the structure of the nNOS heme domain with an *N*-isopropyl-*N*′-hydroxyguanidine bound, we do observe a direct H-bond between the NH-OH group and the carbonyl of Trp587, while the hydroxylated terminal nitrogen can still make an H-bond to the Glu592 side chain. On the basis of the previous discussion, it thus is not surprising that IHG binds well to NOS. What is surprising, however, is that IHG is still a substrate [76% of the activity of L-NHA with nNOS (*21*)] even though its OH group is oriented oppositely with respect to the two other substrates used in this study. To understand how this compound can generate NO with its NH-OH group in an unusual position, we need first to review what is known about the mechanism for the second step of NO biosynthesis.

NO Production from L-NHA. In the first step of NO biosynthesis by NOS, one of the terminal guanidino nitrogens of L-Arg is hydroxylated to give L-NHA, and the reaction is a P450-like monooxygenation reaction utilizing 1 equiv of O_2 and NADPH. However, the mechanism of the second step, generation of NO and citrulline from L-NHA, is unprecedented and requires only one NADPH reducing equivalent and dioxygen. This step of the catalytic cycle is still under active debate.

The early isotope studies (*5*, *6*, *32*) established that (1) L-NHA is an intermediate of NO synthesis from L-Arg, (2) the hydroxylated nitrogen of L-NHA is oxidized to form NO and L-citrulline, (3) both the oxygen in NO and the ureido oxygen in L-citrulline are derived from O_2, and (4) generating 1 mol of NO from L-NHA consumes only 0.5 mol of NADPH. Soon after the discovery that NOSs are heme-containing enzymes, sensible catalytic mechanisms for the second step of NO biosynthesis were proposed (*7*, *33*, *34*) and are summarized in Scheme 2. The consensus of these schemes is that the ferric−hydroperoxy moiety (B in Scheme 2) itself is the active oxidizing species which will not undergo the O−O bond cleavage as in the first step. Rather, the ferric−superoxy moiety (A in Scheme 2) abstracts a hydrogen atom from the OH group of L-NHA, thus forming a hydroperoxy that will attack the central carbon atom of the guanidino group of L-NHA. This leads to an O-radical form of L-NHA (B in Scheme 2) that will form a transient tetrahedral complex with the iron−hydroperoxy species before releasing NO and the byproduct L-citrulline.

On the basis of the mechanistic studies on iron(III) porphyrin-catalyzed oxidation of fluorenone oxime to nitric oxide and fluorenone, Groves and co-workers (*35*) suggested that the second step of the NOS reaction is initiated by formation of a bond between the hydroxyl oxygen atom of L-NHA and the heme iron. The Fe−O bond homolysis will generate an Fe(II) heme and an NHA-derived iminoxy radical

Scheme 2

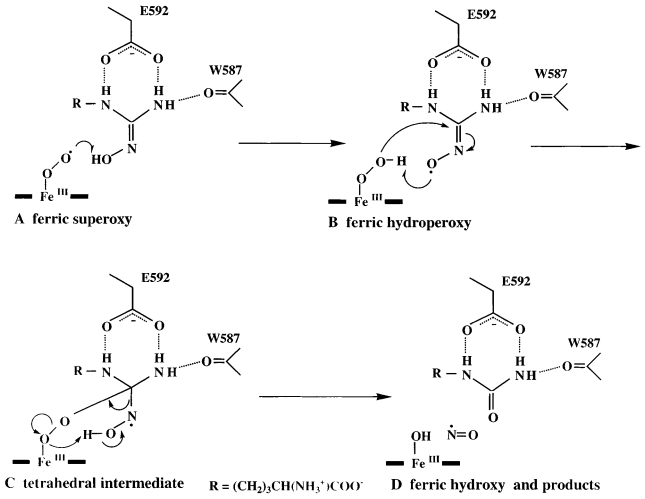

Scheme 3

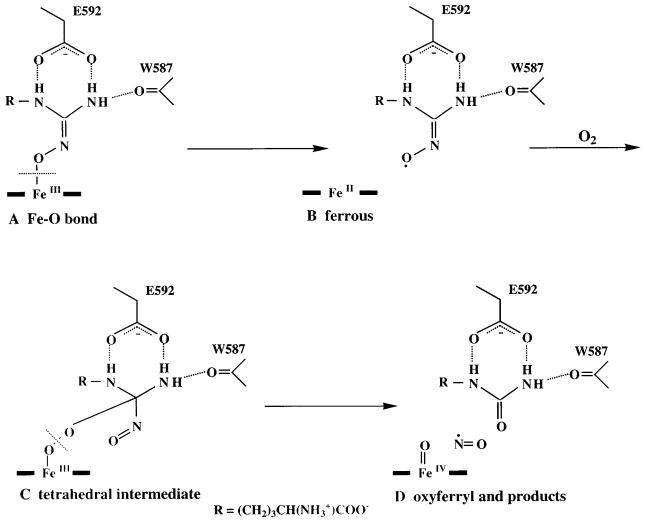

(B in Scheme 3). O_2 binds to the ferrous iron to give a ferric−superoxy species which reacts with NHA radical to form the transient tetrahedral intermediate. The decomposition of the intermediate leads to formation of NO and citrulline.

By analyzing an NHA-bound iNOS crystal structure, Crane et al. (*27*) suggested that due to the steric constraints the NOS active site imposed on the NHA binding, the oxygen of the ferric−superoxy species is too far away from the N^{ω}-OH group of NHA to receive its hydrogen. Instead, the hydroxylated N^{ω} of NHA could be protonated and becomes a hydrogen donor. A recent ENDOR spectroscopic study of L-NHA bound to nNOS (*36*) also supported this notion that the N^{ω} atom is closer to the heme and, therefore, a better candidate as the hydrogen donor. Density functional theory calculations on L-NHA (*37*) indicated if a charged, electron-delocalized guanidinium is the enzyme-bound form of L-NHA, the N-radical would be almost as stable as an O-radical, making the N^{ω} atom an attractive hydrogen donor.

Silverman's laboratory (*38*) recently provided experimental evidence indicating that direct hydrogen atom abstraction from the OH group of N^{ω}-hydroxyarginine is not relevant to the formation of NO from L-NHA. Two NHA analogues, *N-tert*-butyloxy-L-arginine and *N*-(3-methyl-2-butenyl)oxy-L-arginine, were synthesized and proved to be substrates for

Scheme 4

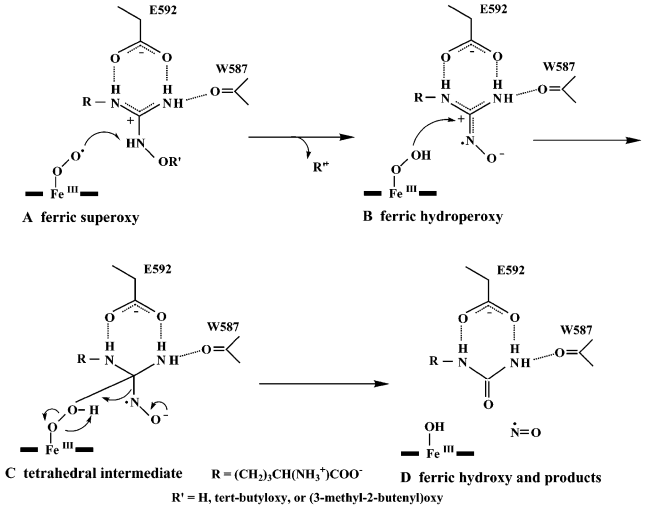

Scheme 5

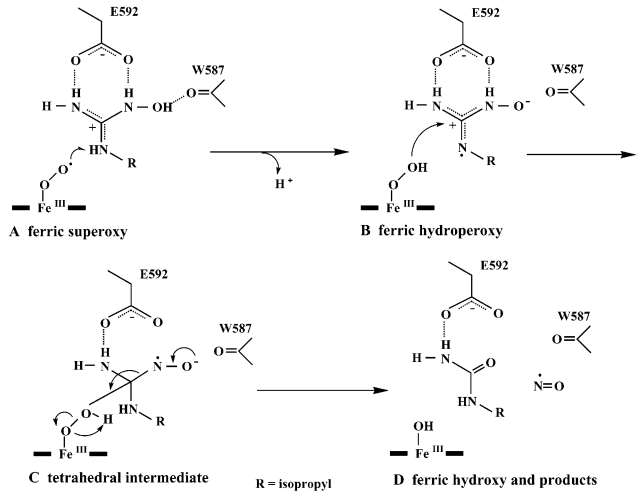

NO formation, although there is no hydrogen attached to the oxygen. The mechanism based on an N-radical intermediate of L-NHA was thus proposed and is shown in Scheme 4.

Mechanistic Implications Based on the Structure of N-Isopropyl-N′-hydroxyguanidine. That the OH group in *N*-isopropyl-*N*′-hydroxyguanidine is located even farther from the heme iron speaks against the Fe−O ligation bond formation shown in Scheme 3 and lends support to the mechanism wherein the N^{ω} atom is the source of the hydrogen atom supplied to the ferric−superoxy species (Scheme 4). In the case of hydroxyguanidine, being charged and electron-delocalized as in hydroxyarginine, all three nitrogen atoms are equivalent and hydrogen-bearing. The alkyl-substituted nitrogen NE is protonated and thus is capable of donating hydrogen to ferric−superoxy species during turnover. A hydrogen-bearing nitrogen atom in the vicinity of ferric−superoxy species appears to be the key feature for a potential hydroxyguanidine substrate of NOS and does not have to be the one bearing the OH group. The location of the hydroxyl group, pointing either to the Gly586 backbone amide or to the Trp587 carbonyl, appears not to be that critical to NO formation. Once the hydrogen is abstracted from a nitrogen, the resulting ferric−hydroperoxy species is a good nucleophile which will attack the central

carbon of guanidinium, leading to NO release, as illustrated in Scheme 5. It is noteworthy that the central carbon atom of the guanidine group still remains close enough to the heme iron, 4.9 Å in IHG versus 4.5 Å in NHA, no matter what orientation the NH-OH group adopts. This is important because in the second step of NO synthesis it is this very carbon atom which undergoes attack by the ferric−hydroperoxy species, the C−N bond being broken, and an oxygen eventually attached to this carbon to give the urea (citrulline in the case of hydroxyarginine) byproduct and release NO.

The discovery of the *N*-alkyl-*N*′-hydroxyguanidines and *N*-aryl-*N*′-hydroxyguanidines (*19*−*21*) as non-amino acid substrates for NOS has created opportunities in finding a new class of NO donors. The novel binding mode of *N*-isopropyl-*N*′-hydroxyguanidine not only helps us understand the mechanism of the second step of NOS catalytic reactions but also provides new clues as to what structural features are essential for a compound to be a NOS substrate. The knowledge base gathered from these studies may eventually aid in searching and designing effective isoform-selective NOS substrates.

ACKNOWLEDGMENT

We gratefully acknowledge the Stanford Synchrotron Radiation Laboratory staff for their assistance during data collection.

REFERENCES

1. Moncada, S., Palmer, R. M. J., and Higgs, E. A. (1991) *Pharmacol. Rev. 43*, 109−142.
2. Dinerman, J. L., Lowenstein, C. J., and Snyder, S. H. (1993) *Circ. Res. 73*, 217−222.
3. Kerwin, J. F., Jr., Lancaster, J. R., Jr., and Feldman, P. L. (1995) *J. Med. Chem. 38*, 4343−4362.
4. Nathan, C. (1997) *J. Clin. Invest. 100*, 2417−2423.
5. Stuehr, D. J., Kwon, N. S., Nathan, C. F., Griffith, O. W., Feldman, P. L., and Wiseman, J. (1991) *J. Biol. Chem. 266*, 6259−6263.
6. Leone, A. M., Palmer, R. M., Knowles, R. G., Francis, P. L., Ashton, D. S., and Moncada, S. (1991) *J. Biol. Chem. 266*, 23790−23795.
7. Griffith, O. W., and Stuehr, D. J. (1995) *Annu. Rev. Physiol. 57*, 707−736.
8. Bec, N., Gorren, A. C., Voelker, C., Mayer, B., and Lange, R. (1998) *J. Biol. Chem. 273*, 13502−13508.
9. Li, H., Raman, C. S., Martasek, P., Masters, B. S. S., and Poulos, T. L. (2001) *Biochemistry 40*, 5399−5406.
10. Hurshman, A. R., Krebs, C., Edmondson, D. E., Huynh, B. H., and Marletta, M. A. (1999) *Biochemistry 38*, 15689−15696.
11. Wei, C. C., Wang, Z. Q., Wang, Q., Meade, A. L., Hemann, C., Hille, R., and Stuehr, D. J. (2001) *J. Biol. Chem. 276*, 315−319.
12. Schmidt, P. P., Lange, R., Gorren, A. C., Werner, E. R., Mayer, B., and Andersson, K. K. (2001) *J. Biol. Inorg. Chem. 6*, 151−158.
13. Masters, B. S. S., McMillan, K., Sheta, E. A., Nishimura, J. S., Roman, L. J., and Martasek, P. (1996) *FASEB J. 10*, 552−558.
14. Abu-Soud, H. M., and Stuehr, D. J. (1993) *Proc. Natl. Acad. Sci. U.S.A. 90*, 10769−10772.
15. Crane, B. R., Arvai, A. S., Ghosh, D. K., Wu, C., Getzoff, E. D., Stuehr, D. J., and Tainer, J. A. (1998) *Science 279*, 2121−2126.
16. Fischmann, T. O., Hruza, A., Niu, X. D., Fossetta, J. D., Lunn, C. A., Dolphin, E., Prongay, A. J., Reichert, P., Lundell, D. J., Narula, S. K., and Weber, P. C. (1999) *Nat. Struct. Biol. 6*, 233−242.
17. Li, H., Raman, C. S., Glaser, C. B., Blasko, E., Young, T. A., Parkinson, J. F., Whitlow, M., and Poulos, T. L. (1999) *J. Biol. Chem. 274*, 21276−21284.
18. Knowles, R. G., Palacios, M., Palmer, R. M. J., and Moncada, S. (1989) *Proc. Natl. Acad. Sci. U.S.A. 86*, 5159−5162.
19. Dijols, S., Perollier, C., Lefevre-Groboillot, D., Pethe, S., Attias, R., Boucher, J. L., Stuehr, D. J., and Mansuy, D. (2001) *J. Med. Chem. 44*, 3199−3202.
20. Renodon-Corniere, A., Dijols, S., Perollier, C., Lefevre-Groboillot, D., Boucher, J.-L., Attias, R., Sari, M.-A., Stuehr, D., and Mansuy, D. (2002) *J. Med. Chem. 45*, 944−954.
21. Xian, M., Fujiwara, N., Wen, Z., Cai, T.-W., Kazuma, S., Janczuk, A. J., Tang, X.-P., Telyatnikov, V. V., Zhang, Y.-X., Chen, X.-C., Miyamoto, Y., Taniguchi, N., and Wang, P. G. (2002) *Bioorg. Med. Chem. 10*, 3049−3055.
22. Moynihan, H. A., Roberts, S. M., Weldon, H., Allcock, G. H., Anggard, E. E., and Warner, T. D. (1994) *J. Chem. Soc., Perkin Trans. 1*, 769−771.
23. Gerber, N. C., and Ortiz de Montellano, P. R. (1995) *J. Biol. Chem. 270*, 17791−17796.
24. Otwinowski, Z., and Minor, W. (1997) *Methods Enzymol. 276*, 307−326.
25. Brunger, A. T., Adams, P. D., Clore, G. M., DeLano, W. L., Gros, P., Grosse-Kunstleve, R. W., Jiang, J.-S., Kuszewski, J., Nilges, M., Pannu, N. S., Read, R. J., Rice, L. M., Simonson, T., and Warren, G. L. (1998) *Acta Crystallogr. D54*, 905−921.
26. Jones, T. A., and Kjeldgaard, M. (1994) *O*, version 5.10, Uppsala University Press, Uppsala, Sweden.
27. Crane, B. R., Arvai, A. S., Ghosh, S., Getzoff, E. D., Stuehr, D. J., and Tainer, J. A. (2000) *Biochemistry 39*, 4608−4621.
28. Vallance, P., Leone, A., Calver, A., Collier, J., and Moncada, S. (1992) *Lancet 339*, 572−575.
29. Boger, R. H., and Bode-Boger, S. M. (2000) *Semin. Thromb. Hemostasis 26*, 539−545.
30. Babu, B. R., Frey, C., and Griffith, O. W. (1999) *J. Biol. Chem. 274*, 25218−25226.
31. Ichimori, K., Stuehr, D. J., Atkinson, R. N., and King, S. B. (1999) *J. Med. Chem. 42*, 1842−1848.
32. Kwon, N. S., Nathan, C. F., Gilker, C., Griffith, O. W., Matthews, D. E., and Stuehr, D. J. (1990) *J. Biol. Chem. 265*, 13442−13445.
33. Marletta, M. A. (1993) *J. Biol. Chem. 268*, 12231−12234.
34. Korth, H.-G., Sustmann, R., Thater, C., Butler, A. R., and Ingold, K. U. (1994) *J. Biol. Chem. 269*, 17776−17779.
35. Wang, C. C.-Y., Ho, D. M., and Groves, J. T. (1999) *J. Am. Chem. Soc. 121*, 12094−12103.
36. Tierney, D. L., Huang, H., Martasek, P., Masters, B. S., Silverman, R. B., and Hoffman, B. M. (1999) *Biochemistry 38*, 3704−3710.
37. Tantillo, D. J., Fukuto, J. M., Hoffman, B. M., Silverman, R. B., and Houk, K. N. (2000) *J. Am. Chem. Soc. 122*, 536−537.
38. Huang, H., Hah, J.-M., and Silverman, R. B. (2001) *J. Am. Chem. Soc. 123*, 2674−2676.
39. Esnouf, R. M. (1997) *J. Mol. Graph. 15*, 132−134.
40. Merritt, E. A., and Bacon, D. J. (1997) *Methods Enzymol. 277*, 505−524.
41. Kraulis, P. J. (1994) *J. Appl. Crystallogr. 24*, 946−950.

BI020417C